Photodiagnosis and Photodynamic Therapy 44 (2023) 103805

Contents lists available at ScienceDirect

Photodiagnosis and Photodynamic Therapy

journal homepage: www.elsevier.com/locate/pdpdt

# A new method based on deep learning and image processing for detection of strabismus with the Hirschberg test

Şükrü Karaaslan [a,*], Sabiha Güngör Kobat [b], Mehmet Gedikpınar [c]

[a] Department of electricity and energy, Organized Industrial Zone Vocational School of Firat University, Elazig, Turkey
[b] Department of Ophthalmology, Hospital of Firat University, Elazig, Turkey
[c] Department of electricity electronics engineering, Firat University Faculty of Technology, Elazig, Turkey

ARTICLE INFO

*Keywords:*
Strabismus
Hirschberg test
Deep learning
Image processing

ABSTRACT

Strabismus is a condition in which one or both eyes do not work in parallel or in harmony. People with strabismus have one eye looking straight ahead while the other eye looks inwards, outwards, upwards or downwards. This condition can affect both eyes. Strabismus is a common eye condition that affects about 4 % of the world's population. Tests such as Hirschberg, Cover and Krimsky are used to detect strabismus. In the Hirschberg test, a light source is held at a distance of 50 cm so that it falls on the centre of each eye. The horizontal and vertical distance between the centre of gravity of the light reflected from the cornea and the centre of the pupil indicates the degree of strabismus. In this study, deep learning and image processing algorithms are used to detect the eye, corneal reflection, iris and pupil on a patient's facial image. Based on the Hirschberg test, the horizontal and vertical shifts for both eyes were measured to determine the patient's degree of strabismus. In this way, the Hirschberg test used in strabismus screening was performed automatically by software. The correct detection of the pupil and the light reflected from the cornea by the algorithm means that the eye has been measured correctly. The software was tested on the facial images of 88 strabismic patients of different sexes and ages. 91 % of the 88 patients, or 80 patients, had their left eye measured correctly. 90 % of the 88 patients, or 79 patients, had their right eye measured correctly. The results for each eye obtained from the correct measurements were found to have an error of maximum $\pm 2^{\circ}$. This error is due to the fact that a real eye is in three-dimensional space, while the digital eye image is in two-dimensional space, and was only observed in the test results of some patients. This algorithm can be tested on patients of all ages and is not affected by morphological differences in the patients' faces. Successful results have been observed experimentally that this newly proposed method can be used in strabismus screening.

## 1. Introduction

Strabismus is one of the most common eye conditions in which one eye is not aligned with the other when looking at an object. It affects approximately 4 % of the world's population [1]. Strabismus can affect an individual's physiological structure as well as their psychological and social life [2]. These patients are more likely to suffer from conditions such as mobility problems and depression. Strabismus can be seen in the setting of thyroid disease, diabetes, increased intracranial pressure, hypertension and some malignancies. Paralytic strabismus may develop secondary to brain tumours, brainstem tumours or vascular lesions and metastatic tumours due to compression. Thyroid-associated orbitopathy (TAO) is one of the most common causes of strabismus in adults [3]. Hypertension and diabetes are other diseases associated with strabismus [4,5]. Therefore, early strabismus screening is important for the management of strabismus in terms of eye health. In strabismus screening, several tests are applied to the patient. Some of these tests are Hirschberg, Cover and Krimsky [6,7].

When deciding on strabismus surgery, the patient's visual acuity, the presence of amblyopia, the presence or absence of fixation and the preferred gaze all influence the timing of surgery. However, making a surgical decision in a single visit is not a correct approach. Repeated measurements are necessary. Especially in paralytic strabismus, it is necessary to wait at least 6 months before making a surgical decision [8].

The cover test is performed by using an opaque or transparent

* Corresponding author.
*E-mail address:* s.karaaslan@firat.edu.tr (Ş. Karaaslan).

https://doi.org/10.1016/j.pdpdt.2023.103805
Received 17 July 2023; Received in revised form 4 September 2023; Accepted 12 September 2023
Available online 22 September 2023

occluder to cover one eye. The occluder covers one eye for a few seconds. While this is being done, the patient is made to look at a target approximately 1/3 metre and 6 m away. The open eye is expected to fixate towards the target and the movement of the open eye is examined with the help of a prism ruler. The same procedure is then repeated for the other eye. As a result of this test, the degree of strabismus in the patient's eyes is expressed in prism units. The Cover test provides complete separation, which gives the maximum deviation angle, and comparison of near deviations. However, it cannot be used in all kinds of deviating movements of the eye [9].

Krimsky test is a Hirschberg-based test. Unlike the Hirschberg test, prisms are used to determine the angle of deviation of the eye. The Krimsky test is recommended for patients with tropias. Thropias is the constant misalignment of the eyes present, but the Krimsky test is not used for patients with phorias. Phorias is a misalignment of the eyes that occurs when the two eyes are not looking at the same object [10].

Recently, there has been an increase in research on strabismus screening tests using image processing and deep learning approaches [11–13]. It has been observed in many studies that Hirschberg or Cover tests used in strabismus screening give effective results when performed through a digital image or video [14,15]. The Hirschberg test can be performed on a digital image and the results can be computed using image processing techniques [16]. However, the Cover test must be performed on a video. Because this test requires closing one of the eyes and watching the movement of the other eye [17]. The more digital images obtained from strabismus patients, the better the software will be trained. The small number of data obtained from strabismus patients is the most important challenge in developing an image processing-based strabismus screening algorithm [18]. There are many strabismus screening methods that work with eye trackers, virtual reality and computer game logic in the digital detection of strabismus [19–22]. Automatic strabismus screening in hospitals, schools and rural areas where the number of patients is high offers the opportunity for early detection and low cost [23]. In addition, the automatic strabismus screening method makes it faster to perform statistical analysis of patients' diagnostic results. In this way, the data can be transferred faster to a digitally based data centre.

This study proposes a new strabismus screening method that automatically performs the Hirschberg test, one of the strabismus screening methods, using deep learning and image processing techniques. This method aims to perform strabismus diagnosis faster and at lower cost by performing the Hirschberg test digitally. Using the degree unit in the Hirschberg test, a mathematical model is developed that reveals the degree-pixel relationship [24]. This proposed method uses a cell phone camera and a cell phone flash as a light source to perform the Hirschberg test. The software aims to provide the most accurate information to the ophthalmologist by detecting the light reflected from the pupil centre and cornea for both eyes and measuring the deviation between the two on the frontal face image taken from strabismus patients. The proposed method was tested on images collected from 88 strabismus patients in the Ophthalmology Department of Firat University Hospital and validated under the control of an ophthalmologist.

## 2. Material method

### 2.1. About ethics

The ethical application to the Rectorate of Fırat University, Faculty of Medicine Dean's Office was approved on 25.05.2023 (document number: 2023/07–42). The data used in this study were collected from patients aged between 2 and 35 years who attended the Ophthalmology Clinic of Firat University Hospital in May, June and July 2023.

### 2.2. Hirschberg test

The Hirschberg test is widely used in patients with strabismus and eye mismatch. In the Hirschberg test, a light source is held at a distance of 50 cm, centred on the root of the nose. The light is reflected from the cornea. In both eyes, the distance between these reflected rays and the centre of the pupil gives the degree of strabismus shift. If the person does not have strabismus, the light reflected from the cornea is seen at the centre of the pupil. In other words, the light reflected from the cornea actually represents the centre of the eye [3].

Fig. 1a and 1b show how the Hirschberg test is applied to a patient and the method of data collection. The data used in this paper were collected from facial images of 88 strabismic patients using the Hirschberg test. Each image in the acquired data has a focal length of 3.99 mm and dimensions of 3024×4032. The RGB colour space images were taken with a 12 megapixels mobile phone camera. The flash on the back of the phone was used as the light source. The patient's face images were captured by having the patient look directly into the camera lens. In strabismus testing, the amount of strabismus shift is expressed in a number of units. These are called degrees and prisms. In the Hirschberg test, 1 mm of shift is equivalent to 7°. Each degree is equivalent to 2 prism diopters. Therefore, each mm shift is approximately 15 prism diopters. In the Hirschberg test, the unit used is usually degrees. In this study, the strabismus shift was expressed in degrees. In addition, the eye images used in this study are presented in grey (binary) format. Fig. 2 shows the light reflected from the cornea of the right and left eye.

### 2.3. Progress

The working scheme of the algorithm developed for strabismus detection is shown in Fig. 3. A 3024×4032 frontal facial image of the patient in RGB colour format is used as input data. A deep learning algorithm (Mediapipe library) identified 478 facial landmarks in the input image. These landmarks are used to detect the right and left eyes and the iris points located in these regions. The algorithm used in the iris regions of interest first detects the light reflected from the cornea, then the pupil and its centre. The deviation between the centroid of the light reflected from the cornea and the centre of the pupil is measured in pixels. The horizontal and vertical deviations for both eyes were converted into degrees using a mathematical model. Finally, the degree of strabismus for both eyes was measured using the developed strabismus detection algorithm. In addition, image processing algorithms were developed using the OpenCV (version 4.5.5.62) library.

### 2.4. Face mesh

In this study, the mediapipe library is used for face detection. This library uses machine learning and deep learning techniques to extract the face mesh. For this deep learning model to work, it is sufficient to have only an image of a human face as input data. Age, skin colour, eye colour and similar differences in the face image do not affect the operation of the deep learning model. This algorithm can find 478 landmarks on a face image. In this way, eyes and eye contours can be detected directly from a face image [5]. This allows us to find the regions of interest on the image using image processing techniques for strabismus detection. The 478 landmarks on a face image are shown in Fig. 4. Each landmark contains horizontal and vertical position information on the face image.

### 2.5. Detection of the eye and its surroundings on the face image

A total of 32 landmark points for the right and left eye on the face image are shown in Fig. 5. Each point contains two parameters for its horizontal and vertical position on the image. For the right eye the landmarks are 33, 246, 161, 161, 161, 160, 160, 160, 159, 158, 157, 157, 173, 133, 155, 154, 153, 145, 144, 163, 7. For the left eye the landmarks are 362, 398, 384, 385, 385, 386, 386, 386, 387, 388, 466, 263, 249, 390, 373, 374, 380, 381, 382.

At each landmark, circles were drawn around the eyes using the

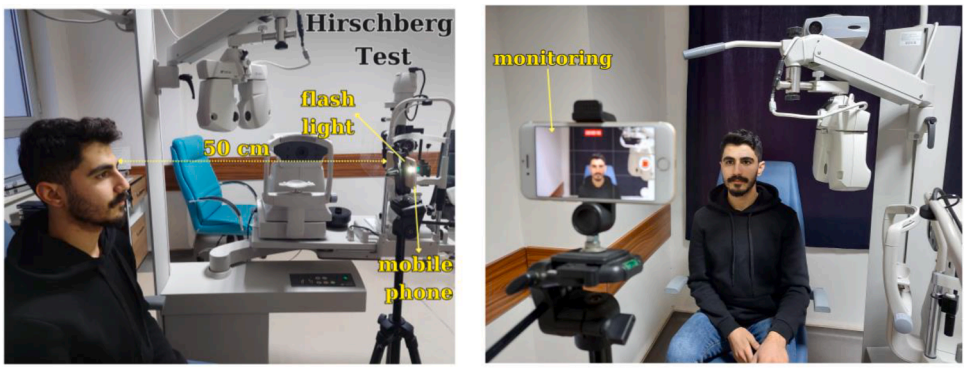


**Fig. 1.** Application of the Hirschberg test and data collection method a) Side view showing camera, light source and distance b) Display of the front face image from the phone screen.

**Fig. 2.** Reflected light on the cornea of both eyes as a result of the Hirschberg test.

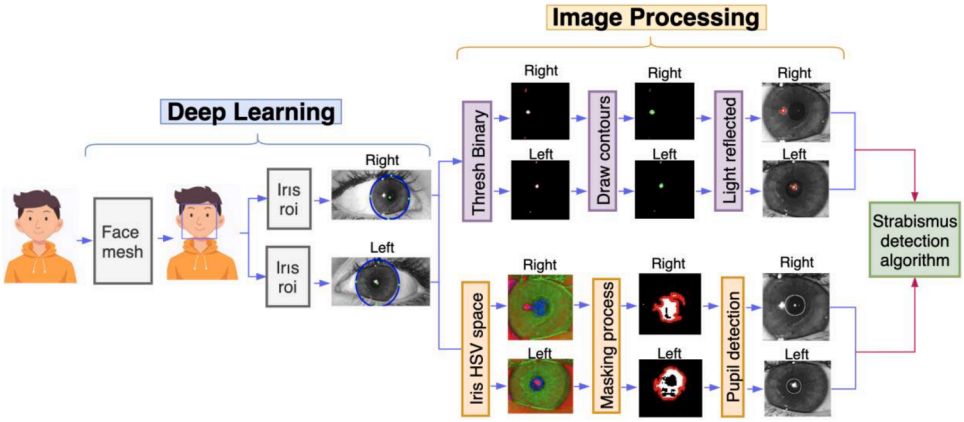


**Fig. 3.** The progression chart of the methods and algorithms used for image segmentation in strabismus detection.

Circle method in the Opencv library, and these circles were connected using the Polylines method. In this way, right and left eye circles were detected in the image. Fig. 6 shows the right and left eye circles obtained from a 3024×4032 face image. This process is not directly necessary for strabismus detection. However, this process becomes important if an interface programme for strabismus detection is to be developed. Errors that may occur in the detection of the eye and its surroundings do not affect the degree of strabismus. In the Hirschberg test, the degree of strabismus is related to the centre of the pupil and the centre of gravity of the light reflected from the cornea.

### 2.6. Detection of iris regions on face image

The 8 landmarks in the face mesh indicate the iris region of the right and left eyes. amongst these landmarks, points 469, 470, 471, 472 contain the coordinates of the iris of the right eye and points 474, 475, 476, 477 contain the coordinates of the iris of the left eye. In Fig. 7, the circle with the smallest radius that can pass through these landmarks is drawn using the minEnclosingCircle method and the centre of this circle is marked as the centre of the iris. The iris landmarks and the centre of the circle surrounding the iris are shown as green circles in the image in Fig. 7. The iris region in the eyes was mostly correctly detected. However, in the case of strabismus detection, the accurate determination of the iris boundary coordinates on the image means that the centre of the iris is also accurately detected. As can be seen in Fig. 7, the centre of the iris is slightly offset from the centre of the pupil. In order to optimise the iris centre, it is necessary to detect the pupil and its centre on the image.

### 2.7. Detection of light reflected from the cornea

To determine the degree of strabismus using the Hirschberg test, the centre of the pupil and the light reflected from the cornea must be detected by image processing [3,4]. The right and left eyes obtained from a face image are shown in Fig. 8a. The iris positions, which are the region of interest (roi) for both eyes, were found as shown in b. A threshold was determined using the Thresh Binary method [8]. Accordingly, pixel values below 200 were set as black and pixel values above this value were set as white and masking was performed. The

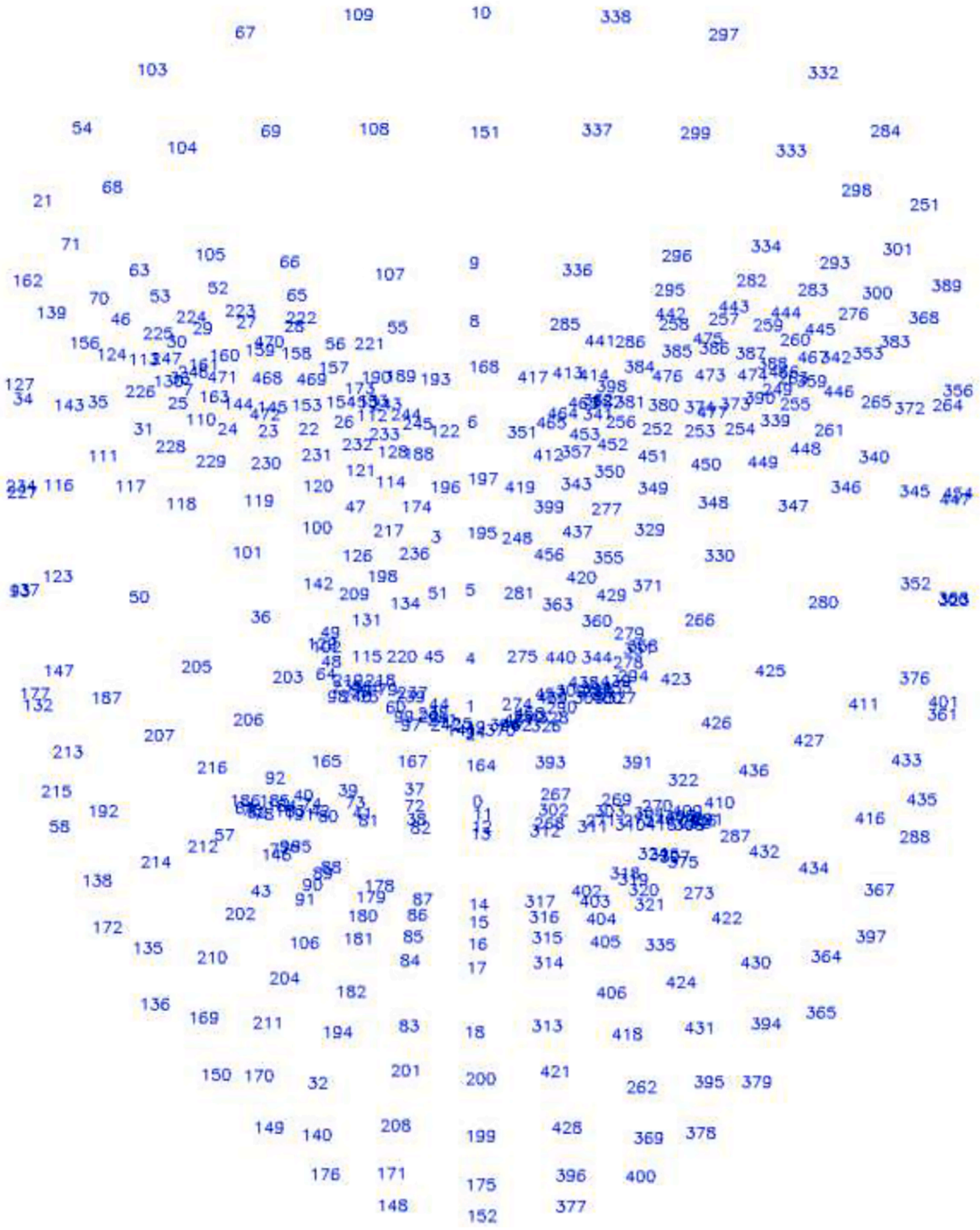

**Fig. 4.** Illustration of landmarks on a face image.

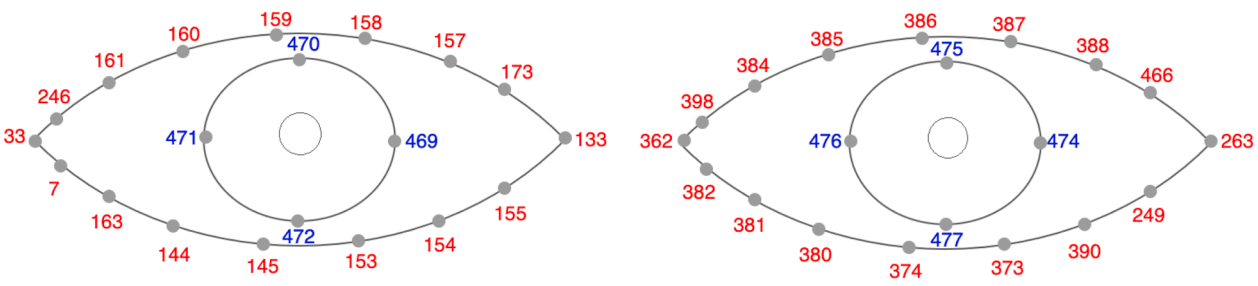


**Fig. 5.** The locations of the eye and iris landmarks in the face mesh.

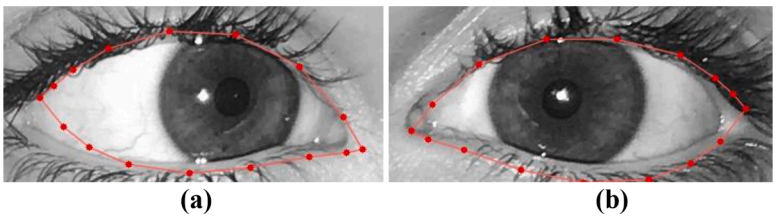


**Fig. 6.** Right and left eye regions a) Right eye contour landmarks b) Left eye contour landmarks.

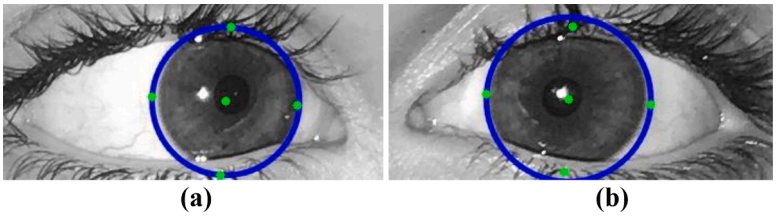


**Fig. 7.** Determination of iris landmarks and iris centre a) Iris landmarks for the right eye b) Iris landmarks for the left eye.

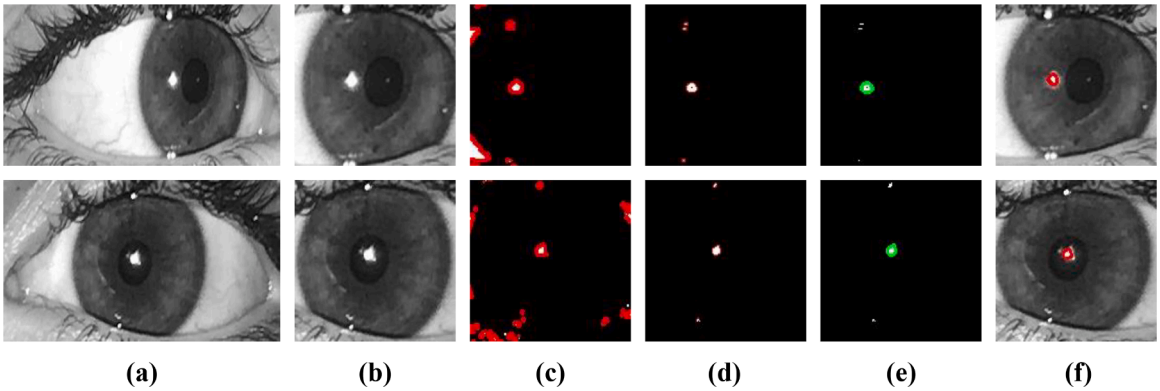


**Fig. 8.** a) Right and left eyes b) Iris regions of interest c) Masked image (threshold = 200) d) Masked image (threshold = 250) e) The contour of the light reflected from the cornea f) Display of the light reflected from the cornea on the iris.

same process was repeated by setting the threshold to 250 and reducing the number of white particles. One of the white particles in image d is the light reflected from the cornea. An algorithm has been developed to find this particle. This algorithm assumes that the white spot closest to the vertical position of the iris centre found previously is the light reflected from the cornea. Using this approach, the light reflected from the cornea in Figure e. is detected and drawn around it in green using the drawContours method. The algorithm is completed by taking the boundary coordinates of the part or contour found in e. and drawing it again on the grey converted version of the same image. The final result is shown in f. and the light reflected from the cornea is detected for both eyes.

## 3. Pupilla detection

The aim of iris detection is to find the centre of the iris, i.e. the centre of the pupil [1]. As can be seen in Fig. 7a and 7b, the points marked as the iris centre can shift in their horizontal or vertical positions. This leads to an inaccurate measurement of the Hirschberg test results. It is therefore necessary to determine the pupil and its centre. When the image is converted to grey (binary) format, the pupil and iris colour pixel values are very close to each other. This makes it difficult to detect the pupil using image processing [6,13]. For this reason, the HSV (hue, saturation, value) colour space, which has been tested to give better results in pupil detection, was preferred in this study [1].

The pictures in Fig. 9 show the steps of the pupil detection process. Although the images in Fig. 9 are different in size, they are shown in 3.1 cm x 3.1 cm dimensions. In a., the iris positions of the right and left eyes are detected by landmarks. In b., the two eye images are represented in the hsv colour space. The image in b. is obtained by cropping 20 % of its length on the x-axis from the right and left parts of the image, and 24 % of its length on the y-axis from the top and bottom parts of the image. This cropping process is implemented as a method in the algorithm. In this way, the image is limited to the pupil and its surroundings. The reason for this cropping is to reduce the different colour tones in and around the iris as much as possible and to create a region of interest around the pupil. Since this operation crops the image, the coordinate information of the main image is lost. To avoid this, the coordinates of the cropped region are added to the necessary variables containing coordinate information in the algorithm. In addition, working in the roi region, which includes the pupil and its surroundings, will minimize the number of contours found with the Contour method. Masking was performed by applying a lower and upper threshold value to the pupil and its surroundings in the HSV colour space. The lower threshold is hsv [30,0,0] and the upper threshold is hsv [179,255,100].

The image obtained as a result of this process is shown in d. By applying the *contourArea* method to the contours in the image in d., the contour with the largest area was assumed to be the pupil and an algorithm working with this approach was developed. In the last stage of pupil detection, the *minEnclosingCircle* method was applied to the

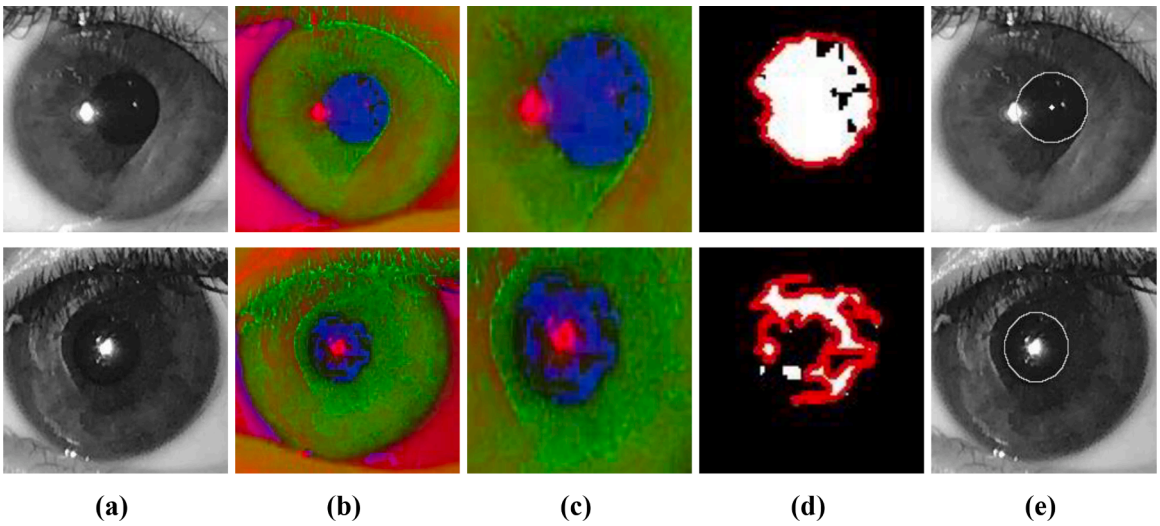


**Fig. 9.** Iris regions for right and left eyes a) Iris regions in grey (binary) format b) Representation of iris regions in HSV colour space for right and left eyes c) Representation of the cropped pupil and its surroundings in HSV colour space d) Masking of the cropped pupilla perimeters e) Representation of the pupil and its centre on the iris.

contour with the largest area, and the pupil and its centre were detected by drawing a circle with the smallest radius enclosing this area. The pupil detected on the image is shown in e. and the coordinates of this region on the x and y axis were obtained. Pupils were detected on iris images of 6 patients and the results are shown in Fig. 10.

### 3.1. Optimization in pupil detection

Some errors may also occur when determining the pupil. These errors are caused by incorrect determination of the exact boundary values of the pupil. Fig. 11. An iris is shown in (a). This image is converted to hsv colour space and shown in (b). As shown in (b), the pupil appears in blue tones due to the effect of reflected light. However, a part of the near region outside the pupil also appears in blue colour tones. This causes the blue tint to extend towards the side of the reflected light from the cornea, causing the pupil boundary to change. As a result, the pupil will be detected incorrectly in such cases. The image resulting from the masking process is shown in (c). On the masked image, the contour that is thought to belong to the pupil, the circle with the smallest radius that can pass through the right-left and lower-upper boundary points, and the centre point of this circle indicate the centre and radius of the pupil. This is shown in (d). However, due to the effect of reflected light, there is an error in the boundaries of the pupil in (d). To correct this situation, a pupil detection optimization algorithm was developed.

The contour segment showing the pupil and the reflected light from the cornea in the masked image is shown in Fig. 12(a). The upper and

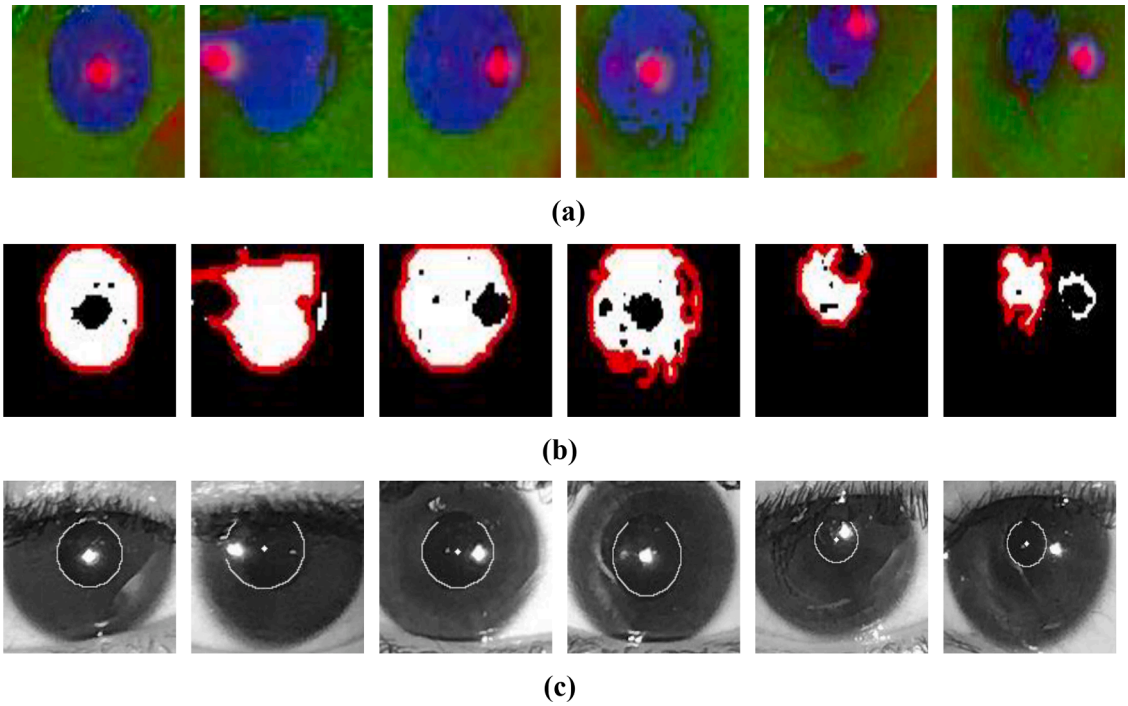


**Fig. 10.** Examples of pupil detection on the images in the data set a) Pupil and its circumference clipped in Hsv colour space b) Masking process in and around the pupil by applying lower and upper threshold values c) Representation of the detected pupil and its centre on the grey format iris image.

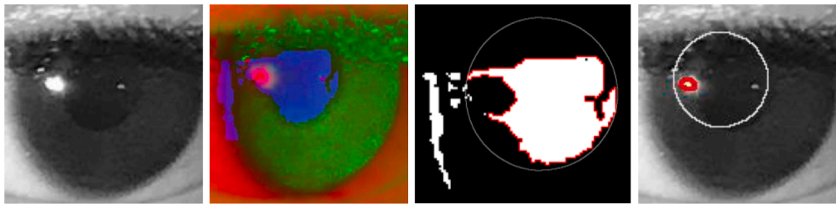


**Fig. 11.** Illustration of pupil detection. a) grey colour format of the iris image b) Representation of iris image in hsv colour space c) Masking operation on the image and display of the lower-upper-right-left border points d) Demonstration of erroneous detection of the pupil.

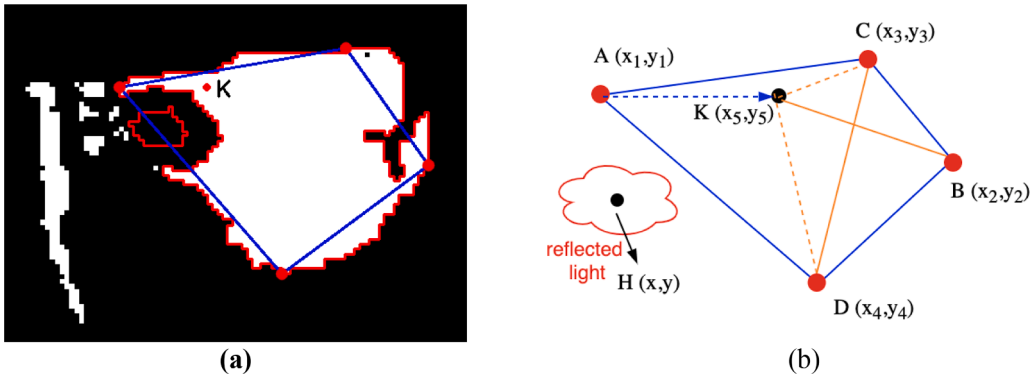


**Fig. 12.** Image of a pupil and its surroundings. a) In the image of the periphery of the pupil where the masking process has been applied, the boundary values of the pupil contour and the display of the contour of the light reflected from the cornea b) schematic representation of the boundary values of the contour of the pupil and the coordinates showing the centre of gravity of the contour of the light reflected from the cornea.

lower boundaries of these contours are symbolized by the letters C and D, the left and right boundaries are symbolized by the letters A and B, and the centre of gravity of the contour showing the reflected light is symbolized by the letter H. Fig. 12(b) shows a schematic representation of these contours. The pupil detection optimization algorithm works on the basis of a mathematical approach that considers the point closest to point H amongst points A,B,C,D as the possible point that changes the boundary of the pupil. For example, in (b), since point A is the closest point to point H, the new position of point A should be point K. Point A is shifted on the horizontal axis. In this case, the upper and lower boundaries of the pupil are points C and D, and the left and right boundaries are points K and B.

Eq. (5), shown in Fig. 12(b), shows the length of AH, Eq. (6), the length of BH, Eq. (7), the length of CH, and Eq. (8), the scalar value of the length of DH.

$$|AH| = \sqrt{(H_x - x_1)^2 + (H_y - y_1)^2} \tag{5}$$

$$|BH| = \sqrt{(H_x - x_2)^2 + (H_y - y_2)^2} \tag{6}$$

$$|CH| = \sqrt{(H_x - x_3)^2 + (H_y - y_3)^2} \tag{7}$$

$$|DH| = \sqrt{(H_x - x_4)^2 + (H_y - y_4)^2} \tag{8}$$

In the last case, the coordinates of points B, C, D from the contours in Fig. 12b are known, but the $K(x_5, y_5)$ coordinates of point K are unknown. An algorithm has been developed to find the coordinates of point K. The points K, B, C, D were considered as the vertices of the rhombus in the circle surrounding the pupil. The diagonals of a rhombus are equal. According to this approach $|KB| = |CD|$ Thanks to the equation, the coordinates of the point K are found and shown in Eq. (9). Since point K is obtained by shifting point A on the horizontal axis, it must be $y_5 = y_1$. The point closest to the centre of gravity of the reflected light can be any of the points B, C and D. In this case, the coordinates of point K are expressed in Eq. (10) for point B, in Eq. (11) for point C, and in Eq. (12) for point D.

$$y_5 = y_1 \text{ and } x_5 = x_2 \mp \sqrt{(x_3 - x_4)^2 + (y_3 - y_4)^2 - (y_1 - y_2)^2} \tag{9}$$

$$y_5 = y_2 \text{ and } x_5 = x_1 \mp \sqrt{(x_3 - x_4)^2 + (y_3 - y_4)^2 - (y_1 - y_2)^2} \tag{10}$$

$$x_5 = x_3 \text{ and } y_5 = y_4 \mp \sqrt{(x_1 - x_2)^2 + (y_1 - y_2)^2 - (x_3 - x_4)^2} \tag{11}$$

$$x_5 = x_4 \text{ and } y_5 = y_3 \mp \sqrt{(x_1 - x_2)^2 + (y_1 - y_2)^2 - (x_3 - x_4)^2} \tag{12}$$

The result of the pupil detection optimization algorithm is shown in Fig. 13a on the masked image. The same detection is shown on a real iris image in Fig. 13b, and pupil boundaries and centre are determined. Point K, which is the new location of point A, is shown in Fig. 13b and the optimization process is concluded.

### 3.2. Strabismus detection

There are some terms used in the detection of strabismus. These are: esotropia, introversion of the eye; exotropia, outward protrusion of the eye; Hypertropia is the upward shifting of the eye and hypotropia is the downward shifting of the eye. The condition in which the ocular muscles of both eyes are considered normal, that is, the absence of strabismus, is called orthophoria. The probabilities of these conditions indicating the direction of strabismus are shown in Fig. 14. The $R_A$, $R_B$, $R_C$, $R_D$, $R_E$ and $R_F$ parameters shown in Fig. 14a represent the horizontal position information of the pupil and iris on the input image for the right eye. $R_A^{'}$,

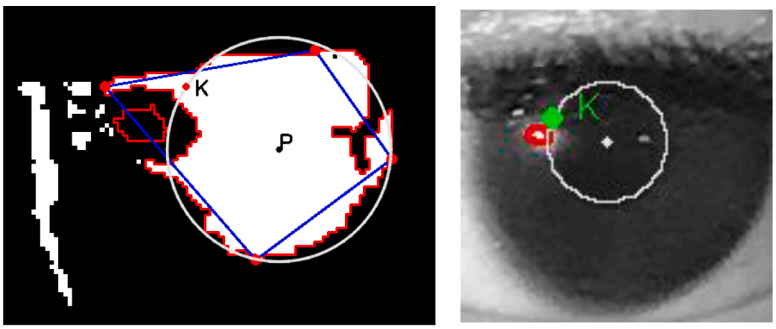


**Fig. 13.** Optimization result in pupil detection a) Display of pupil optimization on masked iris image b) Display of pupil optimization and K-point on the iris image.

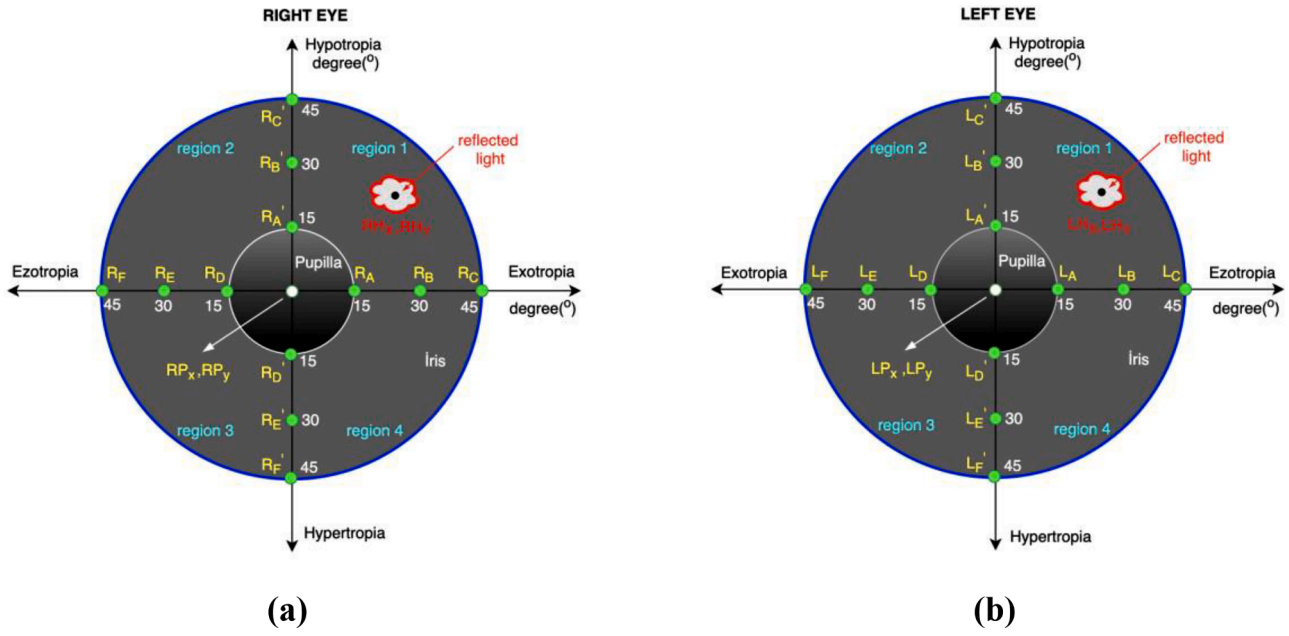


**Fig. 14.** Representation of the strabismus direction in the eyes according to the position of the light reflected from the cornea a) Representation of exotropia, esotropia, hypertropia and hypotropia for the right eye b) Display of exotropia, esotropia, hypertropia and hypotropia for the left eye.

**Table 1**
Success rates of the strabismus detection algorithm in identifying regions of interest.

| Region of interest | Location | Correct detect | Wrong detect | Accuracy % | Location | Correct detect | Wrong detect | Accuracy % |
|---|---|---|---|---|---|---|---|---|
| Eye | Right | 88 | 0 | 100 | Left | 88 | 0 | 100 |
| Iris | Right | 88 | 0 | 100 | Left | 88 | 0 | 100 |
| Pupil | Right | 79 | 9 | 90 | Left | 80 | 8 | 91 |
| Reflected light | Right | 87 | 1 | 98 | Left | 87 | 1 | 98 |

$R_B^{'}$, $R_C^{'}$, $R_D^{'}$, $R_E^{'}$ and $R_F^{'}$ parameters represent the vertical position information of the pupil and iris on the input image for the right eye. $RH_X$ and $RH_Y$ points represent the horizontal and vertical position information on the input image of the light reflected from the cornea. $RP_X$ and $RR_Y$points represent the horizontal and vertical positions of the right pupil centre on the input image. For the left eye, the parameters shown in Fig. 14b are accepted.

The smallest processing unit on an image is the pixel. A mathematical model that reveals the pixel-degree relationship was created to determine the degree of strabismus shift [14]. For the right eye, strabismus is expressed by $RS_x$ horizontally and $RS_y$ vertically; for the left eye, strabismus is expressed by $LS_x$ horizontally and $LS_y$ vertically. According to the magnitude of these parameters, the degree of strabismus was determined, and according to the conditions of being less than or greater than zero, the parameters containing the directional information of the eye shift were determined. Accordingly, the horizontal and vertical radius of an iris corresponds to 45°. The horizontal and vertical projections of the reflected light give the result of strabismus in degrees. Likewise, the axes along which the reflected light is located indicate the direction of the strabismus. For example, in Fig. 14a, there are approximately 20° of exotropia and 20° of hypotropia. The degree and direction of strabismus in the horizontal and vertical position for the right eye are expressed in Eqs. (13) and (14). For the left eye, the degree and direction of strabismus in horizontal and vertical position are expressed in Eqs. (15) and (16).

$$RS_x = \begin{cases} (RH_x - RP_x)x15/(R_A - RP_x), exotropia, \ |RP_x < RH_x \ and \ RP_x < R_A \\ (RH_x - RP_x)x15/(R_B - R_A)+15, exotropia, \ |RP_x < RH_x \ and \ R_A < RH_x < R_B \\ (RH_x - RP_x)x15/(R_B - R_C)+30, exotropia, \ |RP_x < RH_x \ and \ R_B < RH_x < R_C \\ 0 \ , \ none, \ |RP_x = RH_x \\ (RP_x - RH_x)x15/(R_D - RP_x), esotropia, \ |RP_x > RH_x \ and \ RH_x > R_D \\ (RP_x - RH_x)x15/(R_D - R_E)+15, esotropia, \ |RP_x > RH_x \ and \ R_E < RH_x < R_D \\ (RP_x - RH_x)x15/(R_E - R_F) + 30, esotropia, \ |RP_x > RH_x \ and \ R_F < RH_x < R_E \end{cases} \quad (13)$$

$$RS_y = \begin{cases} (RP_y - RH_y)x15/(RP_y - R_A^{'}), hypotropia, \ |RP_y > RH_y \ and \ RH_y > R_A^{'} \\ (RP_y - RH_y)x15/(R_A^{'} - R_B^{'}) + 15, hypotropia, \ |RP_y > RH_y \ and \ R_B^{'} < RH_y < R_A^{'} \\ (RP_y - RH_y)x15/(R_B^{'} - R_C^{'}) + 30, hypotropia, \ |RP_y > RH_y \ and \ R_C^{'} < RH_y < R_B^{'} \\ 0 \ , \ none, \ |RP_y = RH_y \\ (RH_y - RP_y)x15/(R_D^{'} - RP_y), hypertropia, \ |RP_y < RH_y \ and \ RH_y < R_D^{'} \\ (RH_y - RP_y)x15/(R_E^{'} - R_D^{'}) + 15, hypertropia, \ |RP_y < RH_y \ and \ R_D^{'} < RH_y < R_E^{'} \\ (RH_y - RP_y)x15/(R_F^{'} - R_E) + 30, hypertropia, \ |RP_y < RH_y \ and \ R_E^{'} < RH_y < R_F^{'} \end{cases} \quad (14)$$

$$LS_x = \begin{cases} (LH_x - LP_x)x15/(L_A - LP_x), esotropia, \ |LP_x < LH_x \ and \ LP_x < L_A \\ (LH_x - LP_x)x15/(L_B - L_A) + 15, esotropia, \ |LP_x < LH_x \ and \ L_A < LH_x < L_B \\ (LH_x - LP_x)x15/(L_B - L_C) + 30, esotropia, \ |LP_x < LH_x \ and \ L_B < LH_x < L_C \\ 0 \ , \ none, \ |LP_x = LH_x \\ (LP_x - LH_x)x15/(L_D - LP_x), exotropia, \ |LP_x > LH_x \ and \ LH_x > L_D \\ (LP_x - LH_x)x15/(L_D - L_E) + 15, exotropia, \ |LP_x > LH_x \ and \ L_E < LH_x < L_D \\ (LP_x - LH_x)x15/(L_E - L_F) + 30, exotropia, \ |LP_x > LH_x \ and \ L_F < LH_x < L_E \end{cases} \quad (15)$$

$$LS_y = \begin{cases} (LP_y - RH_y)x15/(LP_y - L_A^{'}), hypotropia, \ |LP_y > LH_y \ and \ LH_y > L_A^{'} \\ (LP_y - LH_y)x15/(L_A^{'} - L_B^{'}) + 15, hypotropia, \ |LP_y > LH_y \ and \ L_B^{'} < LH_y < L_A^{'} \\ (LP_y - LH_y)x15/(L_B^{'} - L_C^{'}) + 30, hypotropia, \ |LP_y > LH_y \ and \ L_C^{'} < LH_y < L_B^{'} \\ 0 \ , \ none, \ |LP_y = LH_y \\ (LH_y - LP_y)x15/(L_D^{'} - LP_y), hypertropia, \ |LP_y < LH_y \ and \ LH_y < L_D^{'} \\ (LH_y - LP_y)x15/(L_E^{'} - L_D^{'}) + 15, hypertropia, \ |LP_y < LH_y \ and \ L_D^{'} < LH_y < L_E^{'} \\ (LH_y - LP_y)x15/(L_F^{'} - L_E) + 30, hypertropia, \ |LP_y < LH_y \ and \ L_E^{'} < LH_y < L_F^{'} \end{cases} \quad (16)$$

### 3.3. Statistical analysis

In this study, some regions in and around the eye were detected with image processing techniques. These are the eye contour, iris, corneal reflected light and pupil regions. The success rate in detecting these regions directly affects strabismus detection. As a result of the developed algorithm, the number of correct and incorrect detections of the right and left eye regions of interest of 88 strabismus patients are shown in Table 1.

The graph showing the distribution of 88 strabismus patients in the data set by age and gender is shown in Fig. 15. According to this graph, the age distribution of the patients in the data set is concentrated

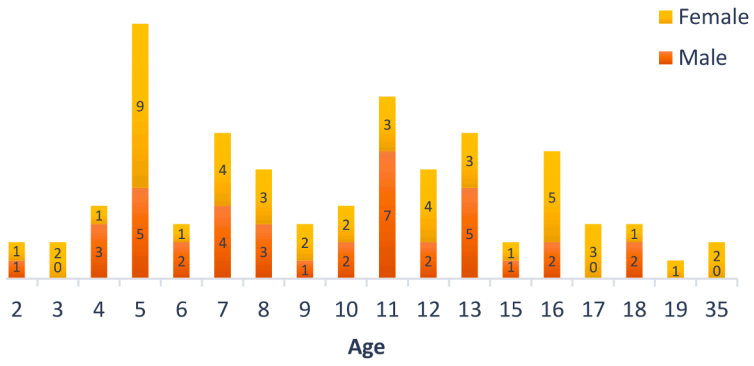


**Fig. 15.** Graph showing the age and gender distribution of strabismus patients in the dataset.

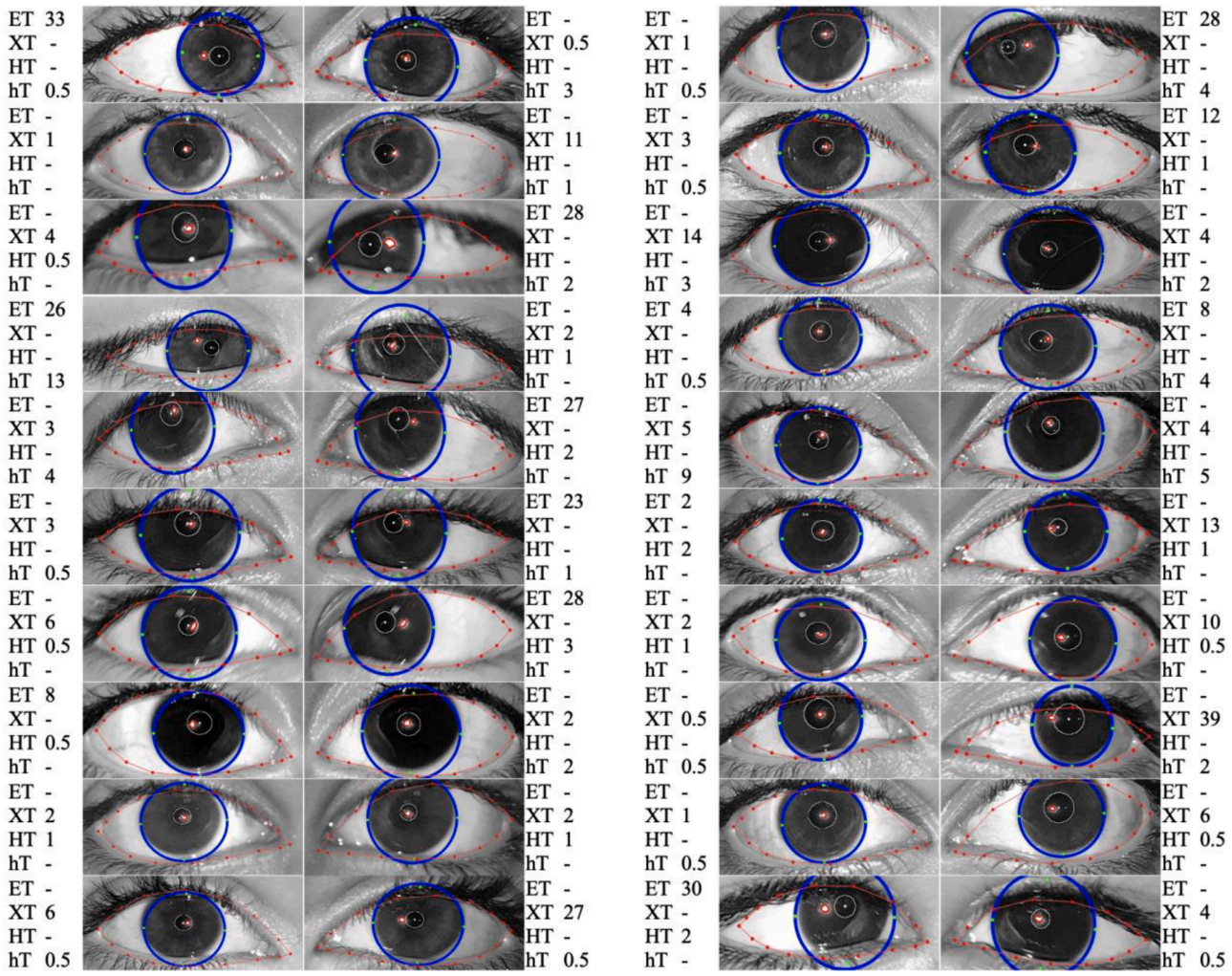


**Fig. 16.** Detection of light reflected from the eye area, iris, cornea and its centre, pupil and its centre on the right and left eyes of 20 strabismus patients in the data set. Display of esotropia (ET), exotropia (XT), hypertropia (HT) and hypotropia (hT) strabismus degrees for both eyes.

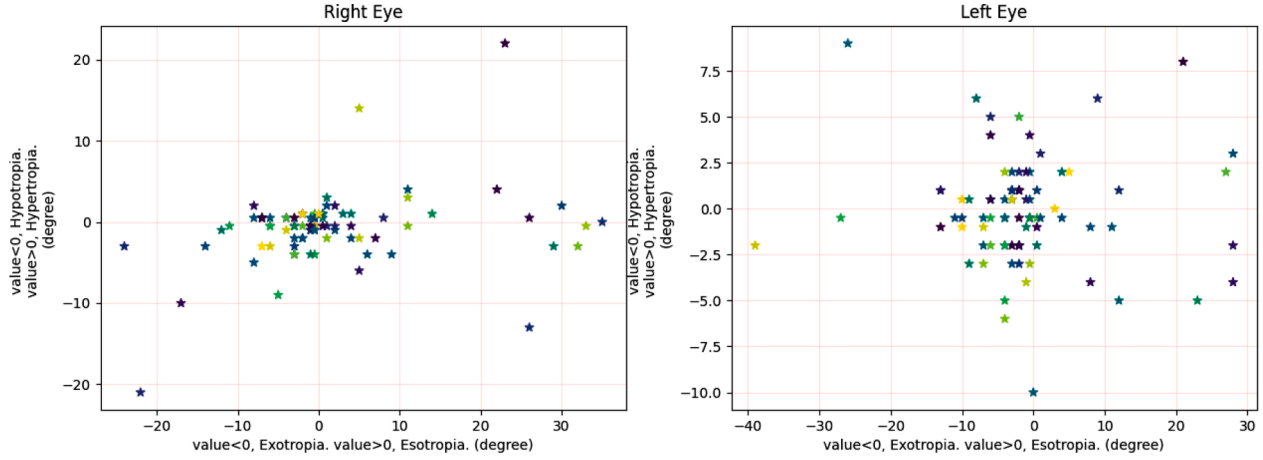


**Fig. 17.** Histogram of the strabismus detection algorithm based on the Hirschberg test, the degrees of strabismus in the right and left eyes of 88 patients in the data set.

between the ages of 2–19. According to gender distribution, 48 of the patients are female and 40 are male. The youngest age of the patients in the data set is 2, and the oldest is 35.

## 4. Conclusions

The algorithm was tested on strabismus images and it was observed that the algorithm gave successful results. These data were used to determine the detection of the eye and its surroundings, the detection of

light reflected from the cornea, the detection of the iris, the detection of the pupil and finally the degree of strabismus such as esotropia (eye turned in), exotropia (eye turned out), hypertropia (eye turned up), hypotropia (eye turned down) for both eyes. The strabismus results for 20 patients are shown in Fig. 16. The results shown in Fig. 16 are abbreviated as esotropia, ET; exotropia, XT; hypertropia, HT; hypotropia, hT and these results are given in degrees for both eyes.

The degree of strabismus of the 88 strabismus patients in the dataset is shown in Fig. 17 for the right and left eye. Each star symbol represents the corresponding eye of the strabismus patient. The horizontal and vertical projections of the asterisk symbol show the degree of strabismus for the same eye.

In this study, if the light reflected from the pupil and cornea is correctly detected in the image, the degree of strabismus is theoretically correct. However, if either of these two regions of interest is incorrectly detected, the degree of strabismus will also be incorrect. According to this approach, the success rate of detecting light reflected from the cornea is higher than the success rate of detecting the pupil for both eyes, as shown in Table 1. Therefore, the success rate of pupil detection also indicates the success rate of strabismus detection for that eye. If the software we have developed can detect the pupil with the light reflected from the cornea, it means that the eye has been measured correctly. According to the data in Table 1, the success rate of pupil detection for the right eye of the patients in the dataset is 90 %. Therefore, the success rate of strabismus detection for the right eye of the patients is 90 %. For the left eyes of the same patients, the success rate for pupil detection is 91 %. Therefore, the success rate for detecting strabismus in the left eye of these patients is 91 %. These rates indirectly represent the number of patients in the dataset that can be measured. Accordingly, the right eye of 80 out of 88 patients was measured correctly. Similarly, the left eye of 79 out of 88 patients was measured correctly.

Just by looking at a person, we can determine the direction of the apparent shift (whether the eye is turned inwards or outwards). But with the Hirschberg or prism closure test, we can determine the quantitative value of the shift. Our gold standard test is the prism closure test. Approximately, 0° indicates the centre of the pupil, 15° indicates the end point of the pupil, 45° indicates the end point of the iris, 30° indicates the midpoint of the end point of the iris and the end point of the pupil. According to this approach, the angle of the eye in one direction is divided into four ranges: 0–15°, 15–30°, 30–45° and more than 45°. The light reflected from the cornea can be in any of these four ranges on the horizontal and vertical axes.

The strabismus detection algorithm measures the difference in pixels between the horizontal coordinate of the light reflected from the cornea and the horizontal coordinate of the pupil centre. If this difference value on the horizontal axis is less than or greater than zero, it indicates the esotropia (the eye is turned inwards) and exotropia (the eye is turned outwards) of that eye. The ratio of this difference on the horizontal axis to the iris radius, multiplied by 45°, gives the degree of strabismus of that eye on the horizontal axis. The difference between the vertical coordinate of the light reflected from the cornea and the vertical coordinate of the pupil centre is measured in pixels. If this difference value on the vertical axis is less than or greater than zero, it indicates hypertropia (the eye is turned up) and hypotropia (the eye is turned down) of that eye. The ratio of this difference on the vertical axis to the iris radius, multiplied by 45°, gives the degree of strabismus of that eye on the vertical axis. The algorithm calculates degrees of strabismus between 0 and 45° as exact values. If the degree of strabismus is outside the range of 0–45°, the algorithm informs us that the degree of strabismus is greater than 45°. If the light reflected from the pupil or cornea is not detected correctly, the ophthalmologist can see this in the software interface. According to the available images, the iris area of a patient under light is approximately 7–10 times larger than the pupil area. If the pupil is incorrectly detected, the algorithm recognises the difference in area between the iris and the pupil and alerts the ophthalmologist.

Although the light reflected from the pupil and cornea was correctly detected in the image in some patients, the degree of strabismus in the eyes was expected to be detected without error; however, there was an error value of maximum ± 2° between these results and the actual results. The reason for this error is that a real eye is in three-dimensional space, whereas an image of an eye is in two-dimensional space. In this study, we set the gold standard error at 3°. If we consider the radius of one eye in the Hirschberg test to be 45°, the gold standard error will affect the patient's degree of strabismus by 3/45, or 6.6 %. In this case, the gold standard error is a value that prevents the ophthalmologist from being wrong.

Some things can be done to increase the success rate of the software algorithm we have developed. A 12 megapixels mobile phone camera was used to collect the data. However, this success rate will increase if a higher resolution camera is used. This is because the more pixels that represent the eye and its surroundings, the more detailed the image will be. In addition, pupils are much easier to detect when a near infrared (NIR) wavelength beam is sent to the eye and its surroundings. This increases the success rate of the software algorithm. Setting the light contrast of the environment in which the patient's face images are taken to a certain value will contribute to the performance of the software algorithm. However, we did not follow such a rule in this study because we wanted to determine the minimum technical conditions under which the strabismus detection algorithm can work. The experimental results show that the developed strabismus detection algorithm gives successful results in the range of 0–45°.

## CRediT authorship contribution statement

**Şükrü Karaaslan:** Writing – review & editing, Writing – original draft, Visualization, Software, Resources, Project administration, Investigation, Funding acquisition, Data curation, Conceptualization. **Sabiha Güngör Kobat:** Methodology, Formal analysis, Validation. **Mehmet Gedikpınar:** Supervision.

## References

[1] X. Huang, et al., An automatic screening method for strabismus detection based on image processing, PLoS One 16 (8) (2021).
[2] Y. Zheng, et al., An automatic stimulus and synchronous tracking system for strabismus assessment based on cover test, in: Proceedings of the International Conference on Intelligent Informatics and Biomedical Sciences (ICIIBMS) 3, IEEE, 2018.
[3] L. Hennein, SL. Robbins, Thyroid-associated orbitopathy: management and treatment, J Binocul Vis Ocul Motil 72 (1) (2022) 32–46.
[4] S. Mishra, et al., Clinical management and therapeutic strategies for the thyroid-associated ophthalmopathy: current and future perspectives, Curr Eye Res 45 (11) (2020) 1325–1341.
[5] K-Ah Park, et al., Acquired onset of third, fourth, and sixth cranial nerve palsies in children and adolescents, Eye 33 (6) (2019) 965–973.
[6] N. Khumdat, P. Phukpattaranont, S. Tengtrisorn, Development of a computer system for strabismus screening, in: Proceedings of the 6th Biomedical Engineering International Conference, IEEE, 2013.
[7] AC. Paglinawan, et al., Detection of three visual impairments: strabismus, blind spots, and blurry vision in rural areas using Raspberry PI by implementing hirschberg, visual field, and visual acuity tests, in: Proceedings of the IEEE 9th International Conference on Humanoid, Nanotechnology, Information Technology, Communication and Control, Environment and Management (HNICEM), IEEE, 2017.
[8] H. Başmak, Extra ocular muscle surgery". Strabismus, Turkish Ophthalmological Society Education Publications, 2008, pp. 287–294.
[9] JM. Holmes, DA. Leske, GG. Hohberger, Defining real change in prism-cover test measurements, Am J Ophthalmol 145 (2) (2008) 381–385.
[10] K.S. Joo, H. Koo, NJu Moon, Measurement of strabismic angle using the distance Krimsky test, Korean J. Ophthalmol. 27 (4) (2013) 276–281.
[11] Su-M Jung, S. Umirzakova, T.K. Whangbo, Strabismus classification using face features, in: Proceedings of the International Symposium on Multimedia and Communication Technology (ISMAC), IEEE, 2019.
[12] J. Santos, I. Frango, Generating photorealistic images of people's eyes with strabismus using Deep Convolutional Generative Adversarial Networks, in: Proceedings of the International Conference on Electrical, Communication, and Computer Engineering (ICECCE), IEEE, 2020.
[13] LK. Cepeda-Zapata, et al., Implementation of a virtual reality rendered in portable devices for strabismus treatment based on conventional visual therapy, in: Proceedings of the 41st annual international conference of the IEEE engineering in medicine and biology society (EMBC), IEEE, 2019.

[14] J.D.S. de Almeida, et al., Computational methodology for automatic detection of strabismus in digital images through Hirschberg test, Comput Biol Med 42 (1) (2012) 135–146.
[15] G. Luo, et al., Using an automated hirschberg test app to evaluate ocular alignment, J VisualExp 157 (2020) e60908.
[16] D. Model, M. Eizenman, An automated Hirschberg test for infants, IEEE Trans. Biomed. Eng. 58 (1) (2010) 103–109.
[17] Y. Zheng, et al., Intelligent evaluation of strabismus in videos based on an automated cover test, Appl Sci 9 (4) (2019) 731.
[18] J.B. Ibarra, et al., Measurement of overall decentration, angle deviation, and prism diopters in categorized strabismus cases using mathematical morphology algorithm, in: Proceedings of the IEEE 9th International Conference on Humanoid, Nanotechnology, Information Technology, Communication and Control, Environment and Management (HNICEM), IEEE, 2017.
[19] U. Saisara, P. Boonbrahm, A. Chaiwiriya, Strabismus screening by Eye Tracker and games, in: Proceedings of the 14th International Joint Conference on Computer Science and Software Engineering (JCSSE), IEEE, 2017.
[20] N.S. Zolkifli, A. Nazari, Tracing of Strabismus Detection Using Hough Transform, in: Proceedings of the IEEE Student Conference on Research and Development (SCOReD), IEEE, 2020.
[21] WA. Mehringer, et al., An image-based method for measuring strabismus in virtual reality, in: Proceedings of the IEEE International Symposium on Mixed and Augmented Reality Adjunct (ISMAR-Adjunct), IEEE, 2020.
[22] N.M. Bakker, et al., Accurate gaze direction measurements with free head movement for strabismus angle estimation, IEEE Trans. Biomed. Eng. 60 (11) (2013) 3028–3035.
[23] T. de Oliveira Simoes, et al., Automatic ocular alignment evaluation for strabismus detection using u-net and resnet networks, in: Proceedings of the 8th Brazilian Conference on Intelligent Systems (BRACIS), IEEE, 2019.
[24] K. Irsch, Optical issues in measuring strabismus, Middle East Afr J Ophthalmol 22 (3) (2015) 265.